Using Solvent Immersion to Fabricate Variably Patterned Poly(methyl methacrylate) Brushes on Silicon Surfaces

Jem-Kun Chen,*,† Chih-Yi Hsieh,‡ Chih-Feng Huang,§ P.-M. Li,‡ Shiao-Wei Kuo,|| and Feng-Chih Chang§

Department of Polymer Engineering, National Taiwan University of Science and Technology, 43, Section 4, Keelung Road, Taipei, 106, Taiwan, Republic of China, Department of Biomechatronics Engineering, National Pingtung University of Science and Technology, PingTung, Taiwan, Department of Applied Chemistry, National Chiao Tung University, Hsinchu, Taiwan, and Department of Materials and Optoelectronic Science, Center for Nanoscience and Nanotechnology, National Sun Yat-Sen University, Kaohsiung, Taiwan

Received May 21, 2008; Revised Manuscript Received September 16, 2008

ABSTRACT: In this paper we describe a graft polymerization/solvent immersion method for generating various patterns of polymer brushes. We used a very-large-scale integration (VLSI) process to generate well-defined patterns of polymerized methyl methacrylate (MMA) on patterned Si(100) surfaces. A monolayer of $Si(CH_3)_3$ groups was first generated to form an inert surface by reacting a hydroxylated Si surface with hexamethyldisilazane in a thermal evaporator. Oxygen plasma was the used to reactivate the patterned surface under a duty ratio of 1:1 using electron beam lithography. The surface-generated oxygen species, such as Si−O and Si−O−O, reacted with the initiator for atom transfer radical polymerization (ATRP) on the patterned hydroxylated surface. The ATRP initiator on the patterned surface was then used for the graft polymerization of MMA to prepare the PMMA brushes. After immersion of wafers presenting lines and dots of these PMMA brushes in water and tetrahydrofuran, we observed mushroom- and brush-like regimes, respectively, for the PMMA brushes with various pattern resolutions.

Introduction

In recent years, the preparation of polymer brushes has emerged as a robust method for creating surfaces exhibiting a wide range of mechanical and chemical properties; in many ways, they act as ideal alternatives to self-assembled monolayers (SAMs).[1−4] One particular advantage that polymer brushes have over spin-coated polymer layers is their stability against solvents or harsh conditions (e.g., high temperatures) because they are bonded covalently to the substrates. The use of polymers as building blocks for surface modification allows the preparation of "smart" or responsive surfaces based on conformational changes in the polymer backbones. These desirable traits have been manipulated in the areas of microelectronics and microfluidics.[5] A range of controlled surface-initiated polymerization techniques have been developed, allowing the formation of (block co)polymer brushes with controlled grafting densities and thicknesses.[6,7] Polymer films patterned using this procedure have been used widely for the fabrication of microelectronic devices[8] or as selective barriers toward etchants.[9] In addition, patterned polymer brushes are routinely produced from the initiator monolayer on a patterned surface.[10−13] While successful, the applicability of these patterned polymer films is restricted by their limited stability with respect to solvents and their tendency to undergo subsequent chemical reactions[14] as well as by difficulties in their preparation over large areas and complicated topographies.[15] To address these latter challenges, Whitesides and co-workers developed microcontact printing[16] for the preparation of patterned SAMs on both planar and curved surfaces.[17] Kang and co-workers prepared SAMs containing patterns of two different initiators, which they subjected to sequential orthogonal polymerization steps.[18] Zhou et al.[19] prepared binary brushes via photoetching and reinitiation, and Luzinov[20] recently reported the use of an imprinted masking layer to form binary brushes.

One goal for the fabrication of patterned macromolecular architectures on surfaces is the realization of complex, often multimolecular, entities in which various interacting organic, biomolecular, and inorganic components are positioned in such a way as to give rise to unique properties and precisely defined structure-dependent functions. The generation of complex patterns in polymer films is traditionally achieved by using a combination of spin-casting and photolithographic techniques.[21] Current commercial lithographic processes can generate patterns with perfection over macroscopic areas and with dimensional control of features, registration, and overlay within tight tolerances and margins. In the past decade, considerable resources have been allocated to the development of exposure tools capable of resolving nanoscale patterns (<30 nm) with the required resolution and overlay capabilities, but relatively modest investments have been made for the development of suitable imaging materials on this length scale. Although these developments are continuing to push the limits of nanomanufacturing, the materials and processes themselves are not amenable to production purposes in their present form.[22] Self-assembling materials used in conjunction with the most advanced exposure tools may enable the current manufacturing practices to be extended to dimensions of 10 nm and less.

Radical-type polymerization methods are used widely for the manufacture of various kinds of commercial products because of the higher stability of radical species in polymerization systems, relative to anionic and cationic species, and the availability of various kinds of monomers. Controlling the reactivity of radical species can be difficult, but recent reports have demonstrated that it is possible to reduce the radical

* To whom correspondence should be addressed. Telephone: +886-2-27376523. Fax: +886-2-27376544. E-mail: jkchen@mail.ntust.edu.tw.
† Department of Polymer Engineering, National Taiwan University of Science and Technology.
‡ Department of Biomechatronics Engineering, National Pingtung University of Science and Technology.
§ Department of Applied Chemistry, National Chiao Tung University.
|| Department of Materials and Optoelectronic Science, Center for Nanoscience and Nanotechnology, National Sun Yat-Sen University.

10.1021/ma801127m CCC: $40.75
Published on Web 10/29/2008

concentration in some systems to provide better control.[23] For example, atom transfer radical polymerization (ATRP) allows the preparation of various kinds of block copolymers, such as diblock-, triblock-, and gradient-type copolymers, with precise control.[24] In addition, it is possible to combine ATRP with other types of polymerization, such as ring-opening metathesis polymerization or anion polymerization, because of the functional group (e.g., halide) that exists at the end of the polymer chain. As a result, many kinds of polymers that are otherwise difficult to synthesize may be prepared by using ATRP.[25] There are many reports describing the preparation of "graft form"-type polymer brushes through ATRP, manipulating its living nature and extending its applicability to a variety of monomers.[26] In addition, Biggs et al.[27] reported the in situ observation of a brush-like polymer structure using atomic force microscopy (AFM) and several reports have described the formation of mushroom-like structures under various conditions.[28,29] Most of these studies have focused on changes in the thickness of the grafted layers; in contrast, the morphological changes of the surface structures in response to changes in solvent have not been characterized very well. In this paper, we report a study aimed at using polymerization to chemically amplify surfaces patterned with a VLSI system into patterned PMMA brushes. We have covalently bonded ATRP initiators onto hydroxylated surface patterns prepared using electron beam lithography and oxygen plasma treatment system, and then amplified the system vertically using ATRP. This surface-initiated polymerization process provides an avenue toward the rapid fabrication of high-resolution patterns of polymers. After immersion in water and tetrahydrofuran (THF), we observed distinct brush- and mushroom-like structures for PMMA brushes patterned with lines and dots.

Experimental Section

Materials. Single-crystal silicon wafers, Si(100), polished on one side (diameter: 6 in.) were supplied by Hitachi, Inc. (Japan) and cut into 2 cm × 2 cm samples. The materials used for graft polymerization, viz., (4-chloromethyl)phenyltrichlorosilane (CMPCS), methyl methacrylate (MMA), copper(I) bromide, and 1,1,4,7,7-pentamethyldiethylenetriamine (PMDETA), were purchased from Aldrich Chemical Co. MMA, PMDETA, and CMPCS were purified through vacuum distillation prior to use. All other chemicals and solvents were of reagent grade and purchased from Aldrich Chemical Co. All solvents were of reagent grade and used without further purification. To remove dust particles and organic contaminants, the Si surfaces were ultrasonically rinsed sequentially with methanol, acetone, and dichloromethane for 10 min each and subsequently dried under vacuum. The Si substrates were immersed in hydrofluoric acid solution (50 wt %) for 5 min at room temperature to remove the silicon oxide film. The hydrofluoric acid-treated substrates were then immersed in the mixture of HNO_3 and H_2O_2 (2:1, mol%) for 10 min and subsequently rinsed with doubly distilled water a minimum of five times to oxidize the Si. This treatment process reduced the water contact angle of the surface from 45 ± 1° to 10 ± 2°.

Immobilization of the Initiator on the Si Surface. The basic strategy for the fabrication of the patterned polymer brushes using the very-large-scale integration (VLSI) process is depicted in Figure 1 and Scheme 1. The Si wafer was treated with hexamethyldisilazane (HMDS) in a thermal evaporator (Track MK-8) at 90 °C for 30 s to transform the hydroxyl groups on the surface of wafer into an inert film of $Si(CH_3)_3$ groups. The photoresist was spun on the HMDS-treated Si wafer at a thickness of 780 nm. Advanced lithography was then used to pattern the photoresist with an array of trenches and contact holes having dimensions between 200 nm to 10 μm after development. The sample was then subjected to oxygen plasma treatment (OPT) using a TCP 9400SE instrument (Lam Research Co, Ltd.) to form hydroxyl groups from the HMDS-treated surface.[30] Plasma treatment of the Si substrates was performed between two horizontal parallel plate electrodes (area: 12 cm × 12 cm). The plasma power supply was set to 300 W at a frequency of 13.5 MHz. The substrate was placed on the bottom electrode with the Si(100) surface exposed to the glow discharge at an oxygen pressure of ca. 5×10^{-3} Torr for a predetermined period of time to form peroxide and hydroxyl peroxide species for the subsequent graft polymerization experiment.[31] Because the glow discharge chamber was purged thoroughly with a continuous oxygen stream prior to ignition, the residual air or water vapor in the chamber had negligible, if any, effect. Oxygen plasma treatment caused the surface to become chemically modified (strongly hydrophilic or polar) only in the areas not covered by the photoresist.[32] The introduction of these polar groups provided a more wettable surface for the preparation of the SAM monolayer for graft polymerization. To immobilize the ATRP initiator (CMPCS), the Si substrate treated with HMDS and oxygen plasma was immersed in a 0.5% (w/v) solution of CMPCS in toluene for 3 h at 50 °C. The CMPCS units assembled selectively onto the bare regions of the Si surface after oxygen plasma treatment, where it reacted with Si−O and Si−O−O species. This procedure resulted in a surface patterned with regions of CMPCS for ATRP and regions of photoresist. The functionalized Si substrates were removed from the solution, washed with toluene for 15 min to remove any unreacted material, dried under a stream of nitrogen, and subjected to surface-initiated polymerization reactions. Finally, the surfaces were dried under vacuum and stored in a dry nitrogen atmosphere.

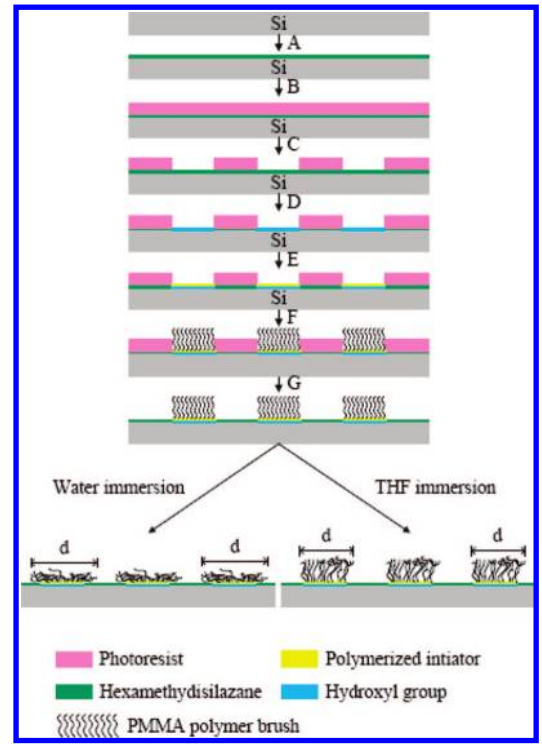

Figure 1. Schematic representation of the process used to fabricate surfaces chemically nanopatterned with PMMA brush. (A) Silicon wafer was treated with HMDS in a thermal evaporator. (B) Photoresist was spin-coated onto the Si surface presenting $Si(CH_3)_3$ groups. (C) Advanced lithography was utilized to pattern the photoresist with arrays of trenches and contact holes on the surface. (D) Oxygen plasma etching was used to chemically modify the exposed regions presenting $Si(OCH_3)_3$ groups and to convert the topographic photoresist pattern into a chemical surface pattern. (E) Initiator, CMPCS, was selectively assembled onto the bare regions of the Si surface. (F) Sample grafting proceeded via surface-initiated polymerization (ATRP) of MMA from the functionalized areas of the patterned SAM. (G) Photoresist was removed through treatment with a solvent.

Surface Initiated Atom Transfer Radical Polymerization. For the preparation of PMMA brushes on the Si−CMPCS surface, MMA (200 mL, 1.87 mol), $Cu^{I}Br$ (18 mg, 0.65 mmol), and

Scheme 1. Synthetic Route toward PMMA Brushes Patterned through OPT, Advanced Lithography, and ATRP on Si Wafers

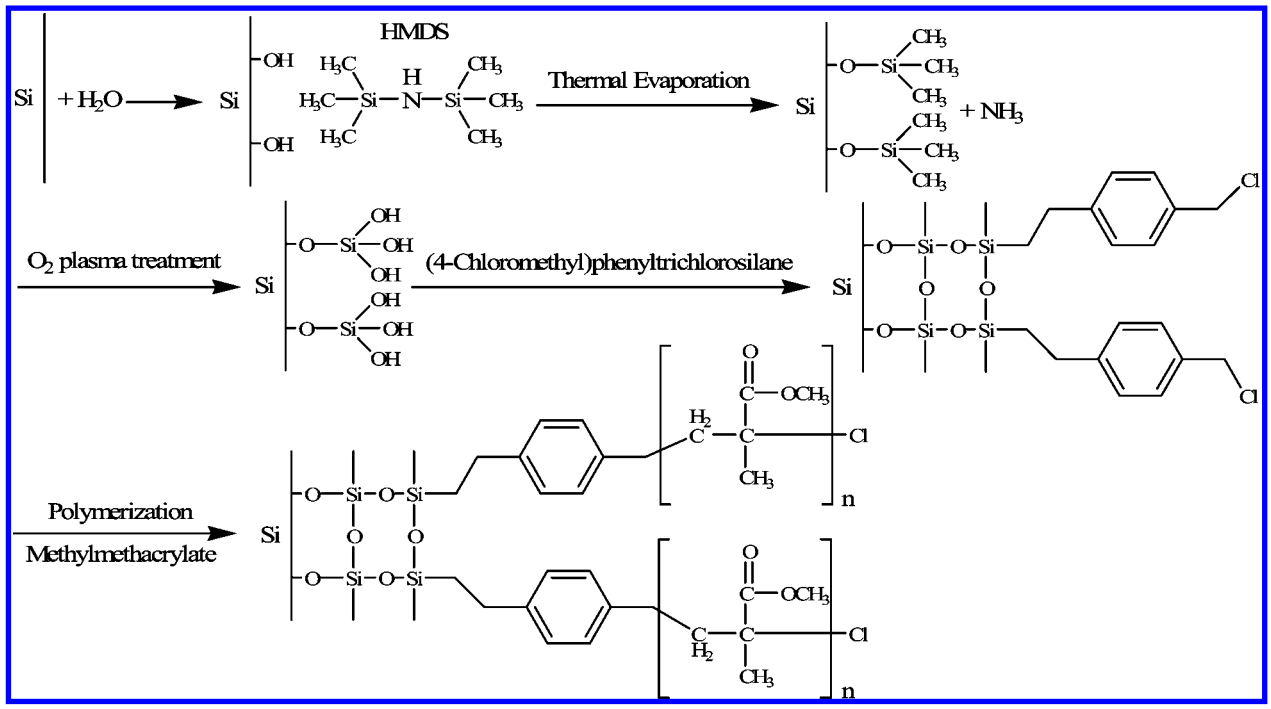

PMDETA (0.2 mL, 0.65 mmol) were added to anhydrous toluene (200 mL). The solution was stirred and degassed with argon for 20 min. The Si−CMPCS substrate was then added to the solution and the temperature was raised to 85 °C. After various polymerization times, the wafers were placed in a Soxhlet apparatus to remove any unreacted monomer, catalyst, and nongrafted material. The remaining photoresist was removed from the HMDS-treated surface by rinsing with solvent, leaving behind the chemically nanopatterned surface. The surfaces were then dried under vacuum at 80 °C for 20 min. The PMMA brushes were immersed in water and tetrahydrofuran (THF) (poor and good solvent for PMMA, respectively) and treated ultrasonically for 3 h before drying under a stream of nitrogen. In addition, samples of "free" PMMA were synthesized in solution under the same conditions ([MMA]:[CMPCS]:[:CuBr]:[PMDETA] = 300:1:1:1; [MMA] = 4.7 M) as those used for grafting polymerization to provide polymers having the same molecular weights of PMMA as the brushes grafted on the Si surface. The "free" PMMA generated in solution from the sacrificial initiator was recovered through precipitation of the reaction mixture into methanol; it was analyzed using gel permeation chromatography (GPC). The monomer conversion was determined gravimetrically. GPC measurements were performed using a VISCOTEK-DM400 instrument and a LR 40 refractive index detector. THF was used as the mobile phase for PMMA; THF containing triethylamine (2 vol %) was used as the mobile phase for PDMAEMA.35 Monodisperse polystyrene standards (Polymer Laboratory, Agilent Co.) were used to generate the calibration curve. Although the exact molecular weight of the polymer grafted on the Si surface is not known, the molecular weight of the graft polymer was expected to be proportional to that of the polymer formed in the solution.[33,34] The polymer-modified Si surfaces were analyzed using ellipsometry (SOPRA SE-5, France), X-ray photoelectron spectroscopy (XPS; PHI 1600 Physical Electronics, USA), a contact angle system (Krüss gmbh, Germany), and AFM (Veeco Dimension 5000 Scanning Probe Microscope).

Surface Energy Calculation. Contact angles were measured using a Kruss-G40 contact angle goniometer. The surface energy was evaluated using the Lifshitz−van der Waals acid/base approach (three-liquid acid/base method) proposed by van Oss et al.[35] This methodology introduces new meanings to the concepts of "apolar" (Lifshitz−van der Waals, γ^{LW}) and "polar" (Lewis acid/base, γ^{AB}), where the latter cannot be represented by a single parameter, such as γ^{p}. Briefly, the theoretical approach follows the additive concept that had been suggested by Fowkes.[36]

$$\gamma = \gamma^{d} + \gamma^{AB} \tag{1}$$

where γ^{d} is the dispersive term of the surface tension. The superscript AB refers to the acid/base interaction. By regrouping the components in eq 1, van Oss et al. expressed the surface energy as

$$\gamma = \gamma^{LW} + \gamma^{AB} \tag{2}$$

Two parameters were created to describe the strength of the Lewis acid and base interactions:

γ_s^+ = (Lewis) acid parameter of surface free energy.

γ_s^- = (Lewis) base parameter of surface free energy.

$$\gamma^{AB} = 2(\gamma_s^+ \gamma_s^-)^{1/2} \tag{3}$$

Van Oss, Good, and their co-workers developed a "three-liquid procedure" (eq 4) to determine the value of γ_S using the contact angle technique.

$$\gamma_L(1 + \cos\theta) = 2[(\gamma_s^{LW}\gamma_L^{LW})^{1/2} + (\gamma_s^+\gamma_L^-)^{1/2} + (\gamma_s^-\gamma_L^+)^{1/2}] \tag{4}$$

To determine the components of γ_S of a polymer solid, three liquids are selected: two of them polar; the third, apolar. Water/ethylene glycol and water/formamide are polar pairs that give good results. The apolar liquid is usually either diiodomethane or R-bromonaphthalene because the LW parameters of the Lewis acid and base are available. The value of γ_S of the Lewis acid and base can then be determined by solving the three equations derived from eqs 3 and 4, simultaneously. By measuring the contact angles of water, diiodomethane, and ethylene glycol, the values of γ_L^{LW}, γ_L^+ and γ_L^- can be obtained.[37]

Results and Discussion

Immobilization of Initiator on the HMDS- and OPT-Treated Si Surface. To prepare polymer brushes on the Si surface, it was necessary for us to immobilize a uniform and

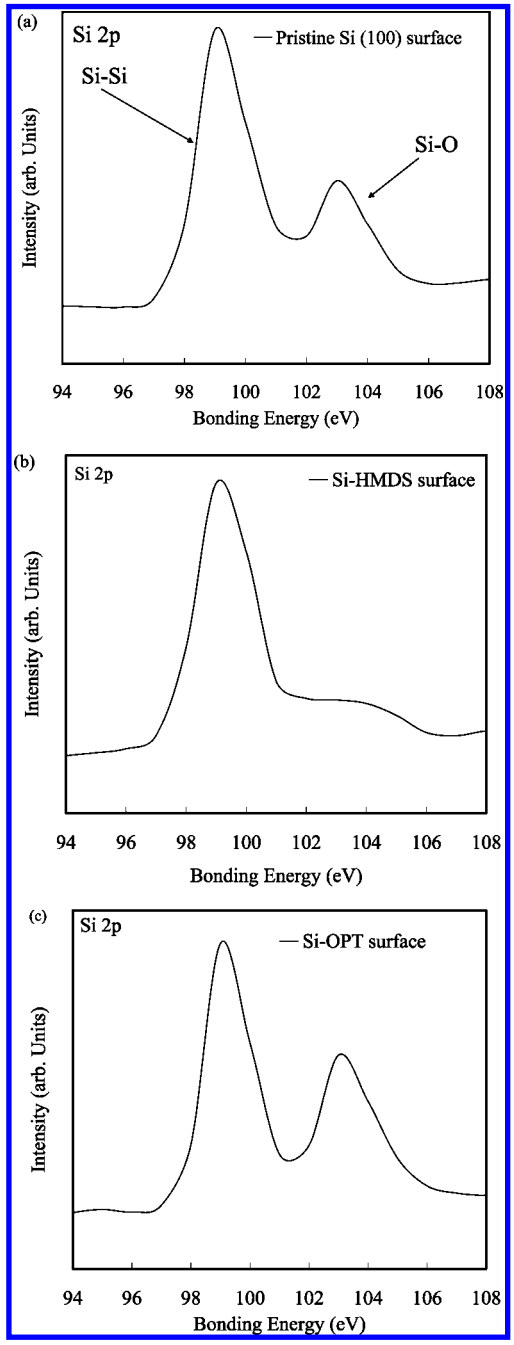

Figure 2. XPS Si 2p core-level spectra of the (a) pristine Si(100) surface, (b) Si−HMDS surface, and (c) Si−HMDS surface after OPT.

dense layer of initiators on the Si surface. The chemical compositions of the pristine Si(100) surface and the Si surfaces at various stages during the surface modification process were determined using XPS. Two peak components at the binding energies (BE) of ca. 99 and 103 eV, attributable to Si−Si and Si−O species, respectively, appear in the Si 2p core-level spectrum of the pristine Si(100) surface (Figure 2a). Treatment of the pristine Si(100) surface with HMDS passivated the native oxide layer and yielded a Si−C surface (Figure 2b). The disappearance of the signal for the Si−O species at a BE of 103 eV confirms that the Si surface was ideally carbon-terminated after HMDS treatment. Treatment of the Si surface with oxygen plasma removed the Si−C layer to activate the Si surface with Si−O species, which appeared as a signal at a BE of 103 eV in Figure 2c. Figure 3a displays the C 1s core-level spectra of the Si−OH surface after being subjected to HMDS,

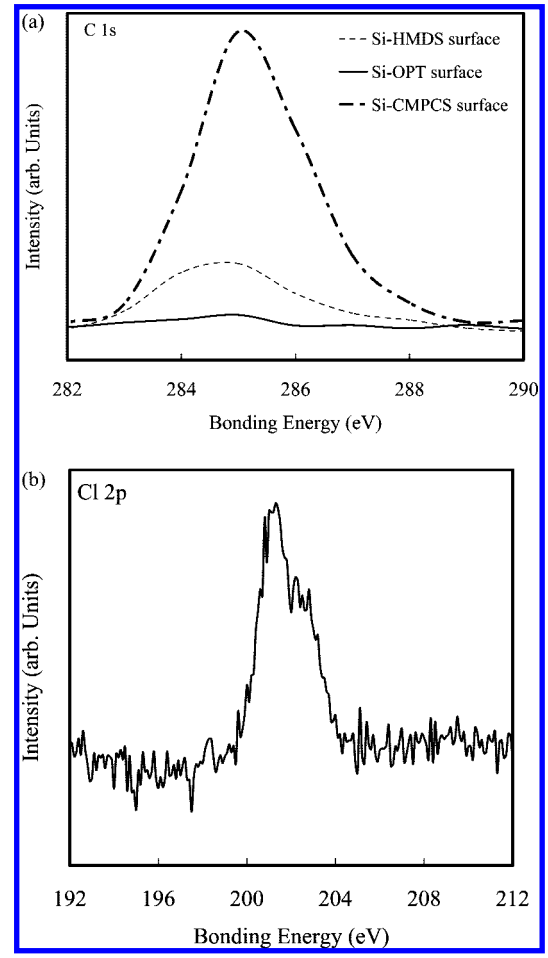

Figure 3. (a) XPS C 1s core-level spectra of the Si−HMDS, Si−OPT, and Si−CMPCS surfaces and (b) XPS Cl 2d core-level spectra of the Si−CMPCS surface.

OPT for 20 s, and CMPCS treatment, respectively. We curve-fitted the C 1s core-level spectra of these alkyl-functionalized silicon surfaces to two peak components having BEs of ca. 283.9 and 284.6 eV, attributable to C−Si and C−H species, respectively.[38] After HDMS treatment, the peaks appeared mainly at BEs of 283.9 and 284.6 eV. We detected extremely small C signals after OPT etching of the Si surfaces. The intensity from C 1s core-level spectrum of the initiator (CMPCS)-functionalized Si surface, curve-fitted with two peak components having BEs at ca. 283.9 and 284.6 eV, increased significantly because of the presence of C−H species of the CMPCS layer on the surface. Additionally, the presence in the Cl 2p core-level spectrum of a signal at a BE of ca. 201.2 eV for the CMPCS-functionalized Si surface (Figure 3b) indicated that the CMPCS species had been immobilized successfully on the Si surface. Table 1 summarizes the surface analysis and surface energy data for the Si−HMDS, Si−OPT, and Si−CMPCS substrate surfaces. The values of the [O]/[Si] and [C]/[Si] ratios of the Si−HMDS surface obtained from XPS analysis were 0.4 and 2.6, respectively, which are in fairly good agreement with their theoretical ratios of 0.5 and 3, respectively. Fairly good agreements also exist between the XPS-derived and theoretical surface compositions of the Si−OPT and Si−CMCPS grafted Si surfaces (Table 1).

Figure 4 display the changes in the C/Si and O/Si atomic ratios of the Si(100) surfaces evaporated with HMDS as a function of the OPT time. The O/Si ratio was determined from the sensitivity factor-corrected C 1s, O 1s, and Si 2p core level peak area ratios obtained at a photoelectron takeoff angle (R) of 75°. The C/Si ratio decreased and the O/Si ratio increased

Table 1. Surface Tension Parameters Calculated from the Advancing Contact Angles for Water, Diiodomethane (DIM), and Ethylene Glycol (EG) on Pristine Si(100), Si−HMDS, Si−OPT, Si−CMPCS, and Si−CMPCS−PMMA Films.

	chemical composition		contact angle (±3°)			surface energy (mN/m)					
sample	[O]/[Si][a]	[C]/[Si][b]	water	DIM	EG	γ^{LW}	γ^{+}	γ^{-}	γ^{AB}	γ	film thickness (±0.5 nm)
Si wafer			39.8	28.2	56.9	30.4	5.7	30.7	26.5	56.9	
Si−HMDS	0.4 (0.5)	2.6 (3)	65.4	42.9	57.6	30.0	6.1	8.2	14.2	44.1	1.1
Si−OPT	1.6 (2)	0.2 (0)	0	20.8	40.5	39.4	2.4	54.8	22.7	62.1	
Si−CMPCS	1.2 (2)	7.2 (4.5)	91	64.9	52.7	32.8	2.6	0.1	0.8	33.6	4.2
Si−CMPCS−PMMA			72.8	57.6	41.4	38.9	1.1	7.0	5.6	44.5	

[a] Determined from XPS core-level spectral area ratio. Values in parentheses are theoretical ratios. [b] Determined from the XPS curve-fitted C 1s core-level spectra. Values in parentheses are theoretical ratios.

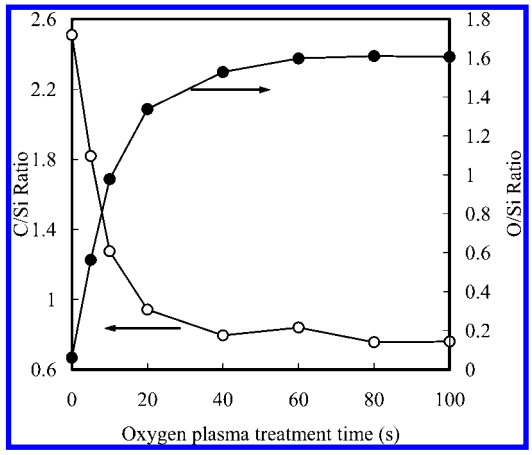

Figure 4. Changes in the O/Si and C/Si atomic ratios of the Si−HMDS surface as a function of the plasma treatment time.

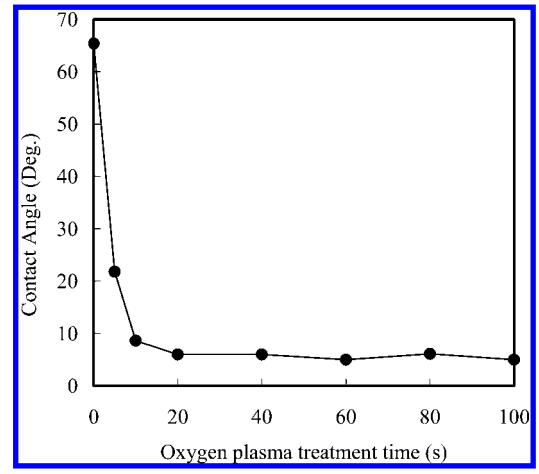

Figure 5. Changes in water contact angles of the Si−HMDS surface as a function of the plasma treatment time.

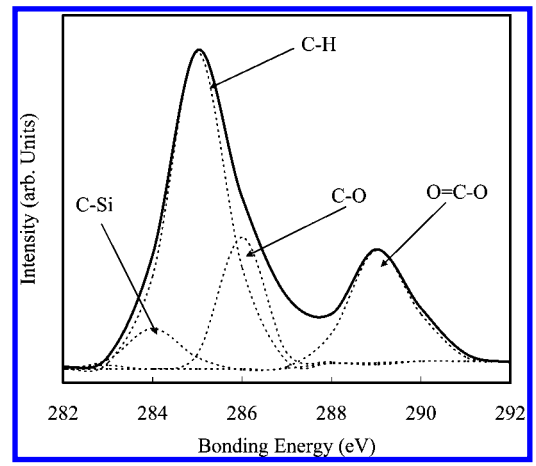

Figure 6. XPS C 1s core level spectra of PMMA brushes grafted from the Si−CMPCS surface for 24 h.

upon increasing the OPT time. These results are similar to those reported previously for the O/Si ratios of Si surfaces.[39,40] The C/Si ratios decreased rapidly during OPT up to a treatment time of ca. 20 s because of the decomposition of the $Si(CH_3)_3$ groups; the C/Si ratio then approached an asymptotic value because of the presence of residual $Si(CH_3)_3$ groups. The O/Si ratios increased rapidly during OPT up to a treatment time of ca. 20 s because of the introduction of oxygen species; the O/Si ratio then approached an asymptotic value. Plasma is used extensively for the treatment of Si wafers, especially for surface cleaning and etching. The idea behind the utilization of the plasma is to create a very reactive gas environment enclosed in a vacuum. Surfaces in contact with the plasma experience interactions that may result in sputtering and chemical reactions caused by highly reactive radicals, low-energy ions, and electrons created in the plasma. Because the chemical properties of Si resemble those of carbon, it can be deduced that OPT of a Si surface, followed by atmospheric exposure, can also introduce some active oxygen species, such as the Si−O and Si−O−O units, that increase the O/Si ratio. We used these active oxygen species for reactions with the initiator of graft polymerization in the subsequent experiments. The introduction of polar groups through plasma treatment also provided a more wettable surface, as indicated by the contact angle data in Figure 5. The contact angle for water decreased rapidly during OPT up to a treatment time of ca. 5 s. The observation suggests that OPT introduced hydroxyl groups extreme rapidly. Table 1 lists the surface energies, obtained from the contact angle data, of the Si−HMDS, Si−OPT, and Si−OPT-CMCPS surfaces. The variation in contact angles of these Si surfaces indicates that the hydrophilicity of the Si surface was readily tuned. The surface energy of the Si−HMDS surface was ca. 44.1 mN/m; after oxygen plasma treatment, the surface energy increased to ca. 62.1 mN/m; immobilization of CMPCS on the Si surface provided a surface energy of ca. 33.6 mN/m. Thus, the Si−OPT surface possessed the highest surface energy because of the hydroxyl groups that had been introduced during the OPT process.

Surface Initiated Polymerization from the CMPCS-Functionalized Silicon Surface via ATRP. We used XPS analysis (Figure 6) to investigate the presence of grafted PMMA brushes on the Si surface. The C 1s core-level spectrum of the PMMA brushes on the Si surface could be curve-fitted to four peak components having BEs of ca. 283.9, 284.6, 286.4, and 288.8 eV, attributable to Si−C, C−H, C−O, and *O*═C−O species, respectively. The presence of new peaks at ca. 286.4 and 288.8 eV confirmed the presence of the PMMA brushes on the Si surface. For the MMA homopolymer, the theoretical values of the [O]/[C] and [CH]:[C−O]:[O═C−C] ratios are 0.4 and 3:1:1, respectively. The corresponding ratios of 0.44 and 2.7:1.2:1 that we obtained from XPS analysis of the Si−CMPCS−PMMA surface are in fairly good agreement with the respective theoretical ratios. The Si surface presenting the PMMA graft layer exhibited a water contact angle of ca. 72.8°, which is equivalent to a surface energy of 44.5 mN/m. Ellipsometry

measurements indicated a large increase from 1.1 to 4.2 nm in film thickness after the growth of the PMMA layer on the Si−CMPCS surface. We performed control experiments on the Si−H, Si−HMDS, and Si−OPT surfaces using conditions similar to those used for the surface graft polymerization via ATRP. In each case, we observed no discernible increase in the thickness of the control surface. These results confirm that the increase in thickness observed was a result of graft polymerization of the CMPCS-functionalized Si surface. Furthermore, because ATRP is a "living" polymerization process, we expected that the thickness of the polymer brushes would increase linearly with the polymerization time and the molecular weight of the graft polymer. We found, however, that the thickness of the PMMA brushes was affected by whether it had been immersed in water or THF. Figure 7a displays the thicknesses of the PMMA brushes grafted for various times onto the Si−CMPCS surfaces, recorded after ultrasonication in water or THF for 3 h. We observe approximately linear increases in thickness of the grafted PMMA layer on the Si−CMPCS surface upon increasing the polymerization time to 12 h, after immersion in either water or THF. The thickness reached a plateau, indicating the formation of mushroom-like regime of the PMMA brushes, after poor solvent (water) immersion of the polymer obtained after polymerization for more than 12 h. In contrast, the thickness of the PMMA brushes grafted on the Si substrate after THF immersion continued to increase upon increasing the polymerization time beyond 12 h, providing a so-called brush-like regime of PMMA brushes. These observations reveal that the PMMA brushes formed mushroom- and brush-like regimes after immersion in water and THF, respectively. In addition, the PMMA layer after water immersion formed the mushroom-like regime when the thickness was less than ca. 20 nm. The thickness of the PMMA brushes after immersion in the good solvent (THF) increase nearly linearly with respect to the polymerization time because of the extension of the PMMA brushes into a brush-like regime.

We obtained additional evidence for the controlled polymerization from "free" PMMA formed from the free initiator. Figure 7b displays the linear relationship between $\ln([M_0]/[M])$ and time, where $[M_0]$ is the initial monomer concentration and [M] is the monomer concentration. The concentration of the growing species remained constant, and first-order kinetics were obtained. Figure 7c presents the relationship between the value of M_n of the free PMMA and the conversion of the MMA monomer. The number-average molecular weight of the "free" PMMA increased linearly upon increasing the monomer conversion. The polydispersity index (PDI, M_w/M_n) of the free PMMA was ca. 1.2. Although we did not determine the exact molecular weight of the polymer grafted on the Si surface, we expected the molecular weight of the graft polymer to be proportional to that of the polymer formed in solution;[34] i.e., we expected the molecular weight of the "free" PMMA formed in the solution to increase linearly with respect to the thickness of the PMMA brushes for various polymerization times. Because of the formation of the mushroom-like regime, the thicknesses of the PMMA brushes after immersion in water reached an approximately constant value while the molecular weight of the "free" PMMA continued to increase. The asymptotic linear relationships verify the brush- and mushroom-like regimes of the PMMA layer. The molecular weight of a PMMA brush on a Si wafer can be determined by measuring the molecular weight of a free polymer because it has been determined previously that their molecular weights are similar.[41] These results obtained after solvent-immersion indicate that the process of surface-initiated ATRP of MMA is controlled between two regimes for PMMA brushes. The grafting density in chains per surface area (D_s, chains/nm^2) may be calculated according to the equation

$$D_s = \mathrm{Th}(d)N_a/M_n$$

where M_n is the molecular weight (g/mol), Th is the thickness (nm), d is the density (g/nm^3), and N_a is Avogadro's number (molecules/mol). Assuming a density of 1.18×10^{-21} g/nm^3 for bulk PMMA, we obtained grafting densities of 0.65 and 0.86 chains/nm^2 from the PMMA brushes grafted for 24 h and then immersed in water and THF, respectively. The two grafting densities indicate that the solvent-immersion process changes the structures of the PMMA brushes on the Si surface. Furthermore, the surface coverage, defined as the amount of the grafted polymer per square meter of surface, is calculated

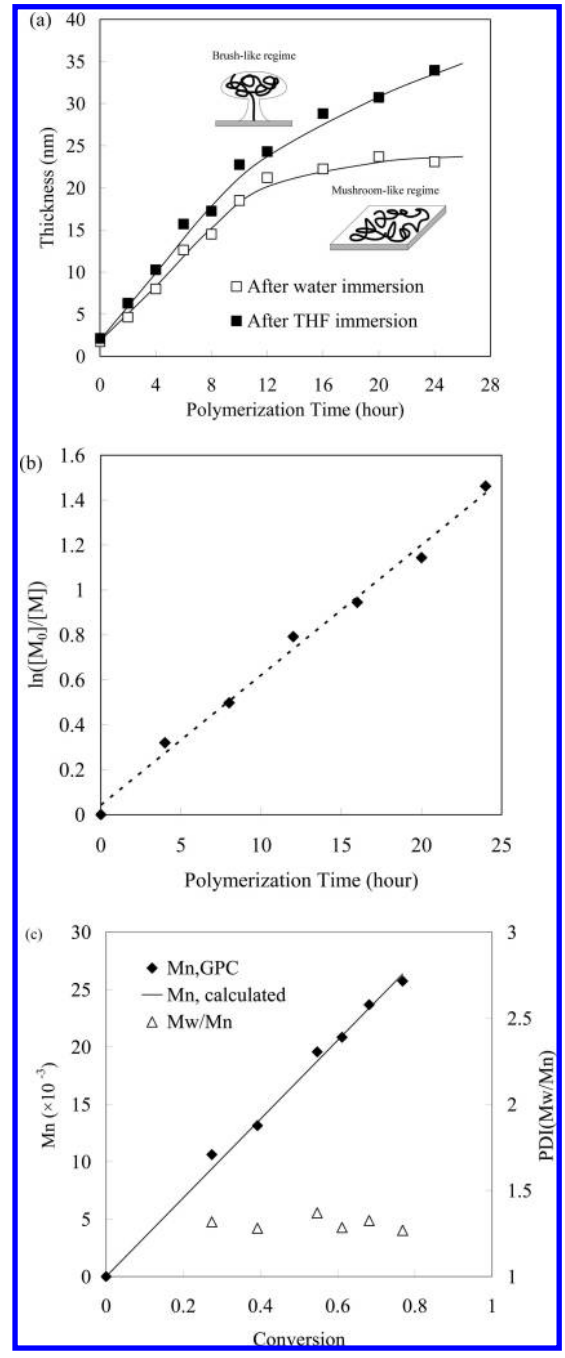

Figure 7. (a) Dependence of the thickness of the PMMA layer, grown from the Si−CMPCS surface via ATRP and then immersed in water or THF, on the polymerization time. (b, c) Relationships between (b) $\ln([M_0]/[M])$ and the polymerization time and (c) the value of M_n of the "free" PMMA formed in solution and the monomer conversion. Reaction conditions: [MMA]:[CMPCS]:[:CuBr]:[PMDETA] = 300:1:1:1; [MMA] = 4.7 M.

from the product of the thickness and the density of the grafted polymer layer.

$$\text{surface coverage} = \text{film thickness} \times \text{density}$$

For simplicity, we used the density of the corresponding bulk polymer (1.18 g/cm^3 for PMMA) as the density of the grafted polymer film. Thus, we calculated surface coverages of 37.4 and 25.4 mg/m^2 for the PMMA brushes obtained after a polymerization time of 24 h and subsequent immersion in THF and water, respectively. These two coverages represent the two types of regimes formed from the PMMA brushes immersed in the poor and good solvents. For the Si−CMPCS−PMMA surface, the surface coverage is comparable to that reported previously for PMMA brushes grown from a native (oxide-covered) Si surface via ATRP.[42] Our calculated grafting densities and surface coverages verified the structural change of the PMMA brushes from the brush- to mushroom-like regimes in water and THF, respectively.

Surface Topography. We used AFM to visualize the topographies of the PMMA brushes grafted onto the Si surfaces through ATRP for 24 h and then subsequently immersed in water and THF. Figure 8a and 8b present representative AFM images of the PMMA brushes after immersion in water and THF, respectively. The root-mean-square surface roughness (R_a) of the pristine Si−H surface was only ca. 0.42 nm. The Si−HMDS and Si−OPT surfaces remained molecularly uniform with values of R_a of ca. 0.51 and 0.55 nm, respectively. After surface treatment with CMPCS, the R_a increased slightly to ca. 1.2 nm. In addition, ellipsometry data indicated that the grafted PMMA film exhibited nanoscopic uniformity in thickness. These results suggest that ATRP graft polymerization proceeded uniformly on the Si−CMPCS surface to give rise to a dense coverage of PMMA. Figure 8a reveals that the MMA polymer chains grafted for 24 h on the Si surface existed as a distinctive overlayer after immersion in water. The surface possessed the mushroom-like structure because of the isotropic or nematic collapse of the PMMA brushed in the presence of the poor solvent.[43] The formation of the islands in Figure 8b probably resulted from the brush-like regime of the PMMA brushes in THF after they had been grafted for 24 h. The values of R_a of the PMMA brushes in their mushroom- and brush-like regimes were 2.876 and 6.758 nm, respectively.

The final step in this strategy was the surface-initiated polymerization of MMA from functionalized areas on the patterned SAM. The incorporation of reactive hydroxyl groups permits after OPT allowed their direct use in the polymerization step. The AFM images in Figure 8c confirm the success of the chemical amplification of the patterned hydroxyl-functionalized SAM into spatially localized polymer brushes. We used lithography processes with positive photoresists to fabricate trenches and contact holes (duty ratio = 1:1) with resolutions ranging from 200 nm to 10 μm. The PMMA brushes were grafted from the Si−CMPCS surfaces of trenches and contact holes to form lines and dots of PMMA brushes. Figure 8c presents the patterned lines of PMMA brushes grafted for 24 h from trenches having a resolution of 5 μm and then immersed in THF. Because of the presence of the mushroom- and brush-like regimes, the widths and radii of the lines and dots functionalized with PMMA brushes had different resolutions after immersion in water and THF, respectively. Figure 9 displays the relationship between the polymerization time of the PMMA brush and the resolution of the lines and dots obtained after immersion in water and THF. The mushroom-like regimes of the PMMA brushes after water immersion enlarged the widths of the lines and the radii of the dots (Figure 9a). Note, however, samples were measured after the surface had been dried. Thus, the PMMA brushes obtained after water

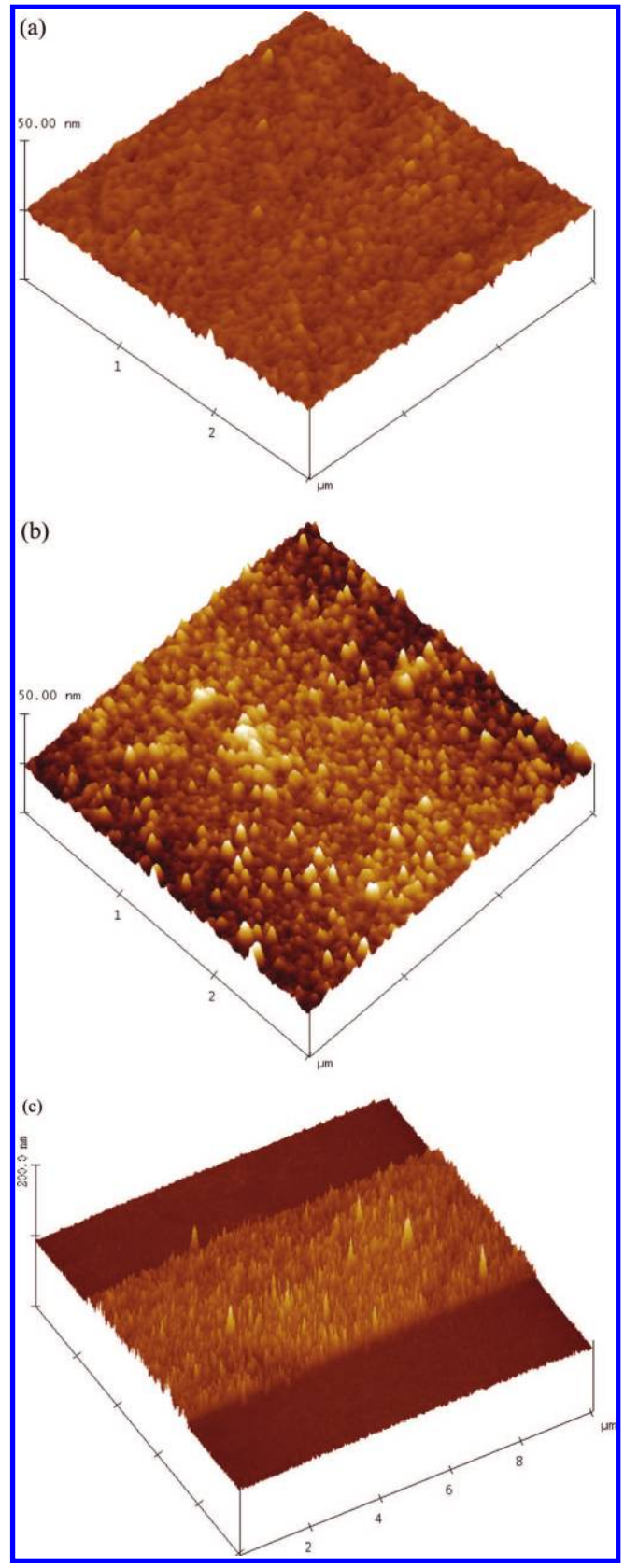

Figure 8. AFM images of PMMA brushes (a, b) obtained after polymerization for 24 h and immersion in (a) water and (b) THF and (c) grafted from 5-μm trenches for 24 h and then immersed in THF.

or THF immersion recovered slightly from their mushroom- or brush-like regimes, respectively, when the polymerization time was greater than 12 h. The widths of the lines and the radii of the dots increased upon increasing the polymerization time for

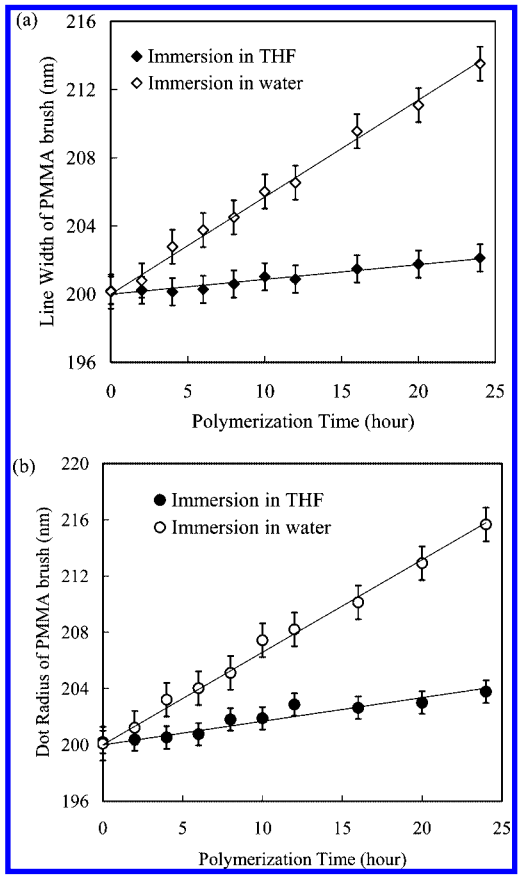

Figure 9. Relationship between the polymerization time of PMMA brushes and (a) the line widths and (b) dot radii of PMMA brushes grafted from 200-nm-resolution trenches and contact holes and then immersed in water and THF.

the PMMA brushes that were immersed in water. The PMMA brushes after THF immersion revealed a slight increase in the widths of the lines and the radii of the dots, verifying the presence of the brush-like regime in this solvent.

Conclusions

We have used the "grafting from" system with ATRP to prepare well-defined dense PMMA brushes on Si wafers. This novel strategy allows the fabrication of patterned polymer brushes from Si surfaces using commercial semiconductor processes. The key feature of this approach is the use of surface-initiated polymerization through OPT to chemically amplify patterned SAMs into macromolecular films. Because this methodology uses commercial photolithographic tools, it provides patterned polymeric thin films having surface properties that are readily controlled on the nanoscale. In addition, the resolution of lines and dots formed from the PMMA brushes can be varied simply by immersion of the wafer in water or THF, which result in brush- and mushroom-like regimes, respectively, for the grafted polymer. Extensions of this strategy to other living and controlled polymerization systems, as well as explorations of the etching and barrier resistance properties of these novel thin films, are under investigation.

Acknowledgment. We thank the National Science Council of the Republic of China for supporting this research financially.

References and Notes

(1) Senaratne, W.; ruzzi, L.; Ober, C. K. *Biomacromolecules* **2005**, *6*, 2427–2448.
(2) Zhou, F.; Huck, W. T. S. *Phys. Chem. Chem. Phys.* **2006**, *8*, 3815–3823.
(3) Jennings, G. K.; Brantley, E. L. *Adv. Mater.* **2004**, *16*, 1983–1994.
(4) Dyer, D. J. *Adv. Funct. Mater.* **2003**, *13*, 667–670.
(5) Hyun, J.; Chilkoti, A. *Macromolecules* **2001**, *34*, 5644–5652.
(6) Edmondson, S.; Osborne, V. L.; Huck, W. T. S. *Chem. Soc. Rev.* **2004**, *33*, 14–22.
(7) Brittain, W. J.; Boyes, S. G.; Granville, A. M.; Baum, M.; Mirous, M. K.; Akgun, B.; Zhao, B.; Blickle, C.; Foster, M. D. *Adv. Polym. Sci.* **2006**, *198*, 125–147.
(8) Lokuge, I.; Wang, X.; Bohn, P. W. *Langmuir* **2007**, *23*, 305–311.
(9) Zamborini, F. P.; Crooks, R. M. *Langmuir* **1997**, *13*, 122–126.
(10) Dong, R.; Krishnan, S.; Baird, B. A.; Lindau, M.; Ober, C. K. *Biomacromolecules* **2007**, *8*, 3082–3092.
(11) Schmelmer, U.; Jordan, R.; Geyer, W.; Eck, W.; Golzhauser, A.; Grunze, M.; Ulman, A. *Angew. Chem., Int. Ed.* **2003**, *42*, 559–563.
(12) Maeng, I. S.; Park, J. W. *Langmuir* **2003**, *19*, 4519–4522.
(13) Kaholek, M.; Lee, W. K.; Ahn, S. J.; Ma, H.; Caster, K. C.; Zauscher, S. *Nano Lett.* **2004**, *4*, 373–376.
(14) Zerushalmi-Royen, R.; Klein, J.; Fetters, L. *Science* **1994**, *263*, 793–795.
(15) Leon, N. L.; Clem, P.; Jung, D. Y.; Lin, W.; Girolami, G. S.; Payne, D. A.; Nuzzo, R. G. *Adv. Mater.* **1997**, *9*, 891–895.
(16) Xia, Y.; Whitesides, G. M. *Angew. Chem.* **1998**, *110*, 568–594.
(17) Jackman, R. J.; Wilbur, J. L.; Whitesides, G. M. *Science* **1995**, *269*, 664–666.
(18) Xu, F. J.; Song, Y.; Cheng, Z. P.; Zhu, X. L.; Zhu, C. X.; Kang, E. T.; Neoh, K. G. *Macromolecules* **2005**, *38*, 6254–6258.
(19) Zhou, F.; Jiang, L.; Liu, W. M.; Xue, Q. *Macromol. Rapid Commun.* **2004**, *25*, 1979–1983.
(20) Liu, Y.; Klep, V.; Luzinov, I. *J. Am. Chem. Soc.* **2006**, *128*, 8106–8107.
(21) Niu, Q. J.; Fréchet, J. M. J. *Angew. Chem.* **1998**, *110*, 685–688.
(22) Gonsalves, K. E.; Merhari, L.; Wu, H.; Hu, Y. *Adv. Mater.* **2001**, *13*, 703–714.
(23) Kamigaito, M.; o, T.; Sawamoto, M. *Chem. Rev.* **2001**, *101*, 3689–3746.
(24) Liu, S.; Weaver, J. V. M.; Tang, Y.; Billingham, N. C.; Armes, S. P.; Tribe, K. *Macromolecules* **2002**, *35*, 6121–6131.
(25) Feng, X. S.; Pan, C. Y. *Macromolecules* **2002**, *35*, 2084–2089.
(26) Wang, J. Y.; Chen, W.; Liu, A. H.; Lu, G.; Zhang, G.; Zhang, J. H.; Yang, B. *J. Am. Chem. Soc.* **2002**, *124*, 13358–13359.
(27) Ishida, N.; Biggs, S. *Langmuir* **2007**, *23*, 11083–11088.
(28) Ohe, C.; Goto, Y.; Noi, M.; Arai, M; Kamijo, H.; Itoh, K. *J. Phys. Chem. B* **2007**, *111*, 1693–1700.
(29) Ishida, N.; Biggs, S. *Macromolecules* **2007**, *40*, 9045–9052.
(30) Chen, J. K.; Ko, F. H.; Hsieh, K. F.; Chou, C. T.; Chang, F. C. *J. Vac. Sci. Technol. B* **2006**, *22*, 3233–3241.
(31) Suzuki, M.; Kishida, A.; Iwata, H.; Ikada, Y. *Macromolecules* **1986**, *19*, 1804–1808.
(32) Stoykovich, M. P.; Müller, M.; Kim, S. O.; Solak, H. H.; Edwards, E. W.; de Pablo, J. J.; Nealey, P. F. *Science* **2005**, *308*, 1442–1446.
(33) Ejaz, M.; Yamamoto, S.; Ohno, K.; Tsujii, Y.; Fukuda, T. *Macromolecules* **1998**, *31*, 5934–5936.
(34) Matyjaszewski, K.; Miller, P. J.; Shukla, N.; Immaraporn, B.; Gelman, A.; Luokala, B. B.; Siclovan, T. M.; Kickelbick, G.; Vallant, T.; Hoffmann, H.; Pakula, T. *Macromolecules* **1999**, *32*, 8716–8724.
(35) Van Oss, C. J.; Ju, L.; Chaudhury, M. K.; Good, R. J. *J. Colloid Interface Sci.* **1989**, *128*, 313–319.
(36) Fowkes, F. M. *J. Phys. Chem.* **1962**, *66*, 382–382.
(37) Drummond, C. J.; Chan, D. Y. C. *Langmuir* **1997**, *13*, 3890–3895.
(38) Yu, W. H.; Kang, E. T.; Neoh, K. G. *J. Phys. Chem. B* **2003**, *107*, 10198–10205.
(39) Da, Y. X.; Griesser, H. J.; Mau, A. W. H.; Schmidt, R.; Liesegang, J. *Polymer* **1991**, *32*, 1126–1130.
(40) Zhang, J.; Cui, C. Q.; Lim, T. B. *Chem. Mater.* **1999**, *11*, 1061–1068.
(41) Rowe-Konopacki, M. D.; Boyes, S. G. *Macromolecules* **2007**, *40*, 879–888.
(42) Mori, H.; Boker, A.; Krausch, G.; Muller, A. H. E. *Macromolecules* **2001**, *34*, 6871–6882.
(43) Zhao, B.; Brittain, W. J. *Prog. Polym. Sci.* **2000**, *25*, 677–710.

MA801127M